Progress In Electromagnetics Research M, Vol. 103, 103–113, 2021

Electrically Small Radiation Pattern Reconfigurable Antenna with Expanded Bandwidth and High Front-to-Back Ratio

Hui-Fen Huang* **and Hong-Long Bu**

Abstract—This paper presents an electrically small antenna ($ka = 0.87$) with ultra-low-profile $0.005\lambda_0$ and six reconfigurable endfire radiation patterns, which cover the entire 360° azimuth plane. An equivalent magnetic dipole and six switchable equivalent electric dipoles achieve the six reconfigurable endfire radiation patterns by switching the ON/OFF states of six PIN diodes. The designing bright point is the dual side printed loop, that is, an Alford loop and six loaded circular arc stubs, which form the equivalent magnetic dipole. This technique can reduce the size by 77% compared with single side printed loop, expand the bandwidth, and produce a strong and uniform near magnetic field, which leads to a high F/B ratio. Compared with published pattern-reconfigurable ESAs with endfire radiation characteristics, the proposed antenna has higher F/B ratio about 35.6 dB, more switchable states and expanded bandwidth. In addition, the measured peak realized gain and radiation efficiency at 1.5 GHz are 3.52 dBi and 77.6%, respectively.

1. INTRODUCTION

With the rapid development and innovations of wireless communication, wireless electronic devices are required to be more compact, integrated, portable, lower cost, smarter, and multifunctional. Reconfigurable antennas become a promising and sustainable solution. In particular, pattern reconfigurable antennas can enhance the anti-interference ability by adjusting the main beam radiation direction in real time. Therefore, they have been widely used in mobile communications, sensor networks, and intelligent transportation systems (ITS) [1–3].

Many pattern reconfigurable antennas have been designed, such as dielectric resonator antenna [4], arc dipoles antenna [5], Yagi-Uda antennas [6], microstrip array antennas [7], near-field resonant parasitic (NFRP) antenna [8], and unilateral planar antennas [9]. The radiation patterns by them were easily reconfigured by switching among the PIN diodes. However, the above antennas are not electrically small, i.e., $ka > 1$, where $k = 2\pi/\lambda_0$, λ is the operational free-space wavelength, and a is the radius of the smallest sphere that encloses the entire antenna system. Therefore, their applications in more compact and small communication systems are very limited.

Recently, pattern-reconfigurable electrically small antennas (ESAs) have also been investigated extensively [10–13]. In [11], a three-state pattern-reconfigurable ESA was developed, consisting of three magnetic NFRP elements and a diode-loaded electric NFRP element. The antenna is electrically small, but it is not a planar structure, including two layers of substrates and an air gap between them. Single layer pattern-reconfigurable planar ESAs are proposed in [12, 13], and they can achieve wide impedance bandwidth and high gain, respectively. However, their reconfigurable endfire radiation patterns cannot cover the entire 360° azimuth range. The F/B ratio of the four antennas is about 7 dB, 17.5 dB, 16.15 dB, and 13.3 dB, respectively. In addition, the bandwidths of the four antennas are 2.7%, 2.73%, 12.9%, and

Received 6 May 2021, Accepted 1 July 2021, Scheduled 8 July 2021
* Corresponding author: Hui-Fen Huang (huanghf@scut.edu.cn).
The authors are with the School of Electronic and Information Engineering, South China University of Technology, Guangzhou, China.

1.32%, respectively. In summary, most pattern-reconfigurable ESAs have relatively narrow bandwidth, few switchable states, and low F/B ratio.

In this paper, we develop a single layer pattern-reconfigurable ESA with expanded bandwidth of 7.3%, high F/B ratio of 35.6 dB, and six switchable endfire radiation states, which cover the entire 360° azimuth plane. The paper is organized as follows. Section 2 is the single layer pattern-reconfigurable ESA design. Section 3 is the simulated performance and experimental validation, and Section 4 is conclusion.

2. PATTERN-RECONFIGURABLE ESA DESIGN

2.1. Antenna Description

The developed pattern-reconfigurable ESA with endfire radiation characteristics is illustrated in Fig. 1. As shown in Fig. 1(a), an Alford loop and a slotted ground with six circular arc stubs are printed on the top and bottom sides of the substrate, respectively. A coaxial cable is used to feed this antenna in the center. The six circular arc stubs and the Alford loop are coupled with each other to produce a miniaturized equivalent magnetic dipole. As shown in Fig. 1(c), the six rectangular slots and PIN diodes on the ground plane can introduce six switchable equivalent electric dipoles. By properly adjusting the key dimensions of the antenna, 180° phase difference and same radiation intensity can be obtained between the six switchable electric dipoles and the magnetic dipole, and then six switchable endfire radiation patterns are achieved. In addition, the circular arc slot on the ground plane is for improving impedance matching and miniaturization. The antenna is made on an F4B substrate with relative permittivity $\varepsilon_r = 2.2$, radius 28 mm, thickness 1 mm, and loss tangent $\tan\delta = 0.0007$. The antenna was designed by ANSYS HFSS, and the optimized parameters are marked in Table 1.

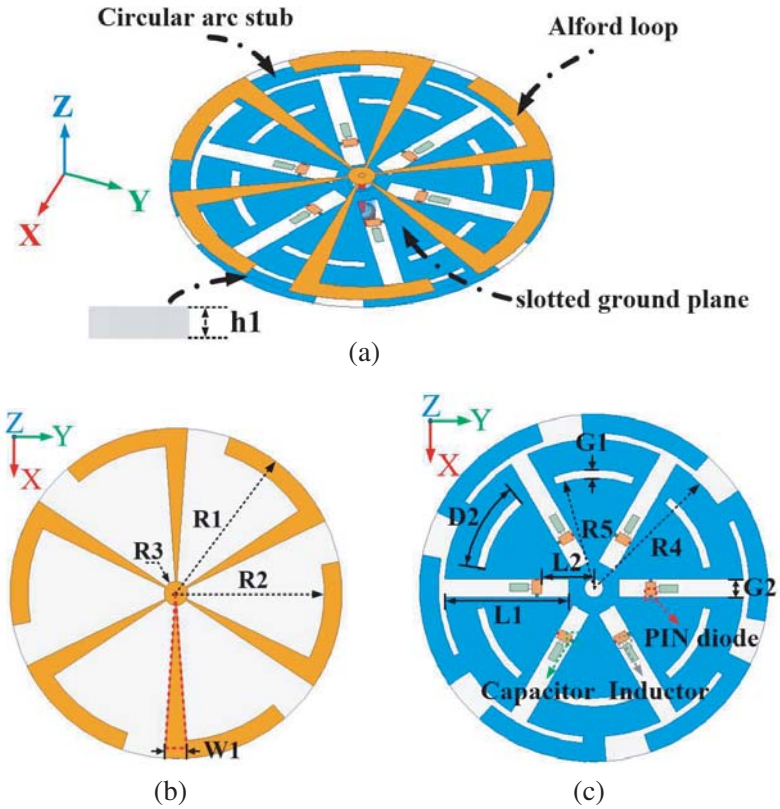

Figure 1. Configuration of single layer pattern-reconfigurable ESA. (a) 3-D view. (b) Top view. (c) Bottom view.

Table 1. Optimized design parameters of the single layer pattern-reconfigurable ESA (mm).

$h1 = 1$	$R1 = 28$	$R2 = 25$	$R3 = 2$	$R4 = 24$
$R5 = 17.8$	$L1 = 20$	$W1 = 3.6$	$G1 = 1.3$	$G2 = 3$
$L2 = 8.4$	$D1 = 41°$	$D2 = 20°$	Null	

2.2. Electrically Small Endfire Radiation Antenna Design

The design process of the electrically small antenna with endfire characteristics is shown in Fig. 2, which mainly includes four steps. For Ant-1, an Alford loop forms the equivalent magnetic dipole. The center frequency is 3.32 GHz, and its radiation pattern is omnidirectional as shown in Fig. 3(a). For Ant-2, six circular arc stubs are loaded on the ground plane of Ant-1. The equivalent magnetic dipole that

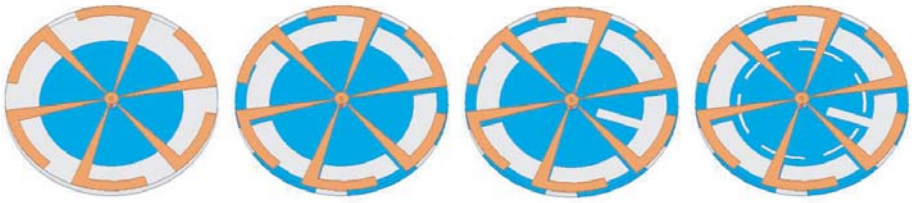

(a) (b) (c) (d)

Figure 2. The design process: (a) Ant-1, (b) Ant-2, (c) Ant-3, (d) Ant-4.

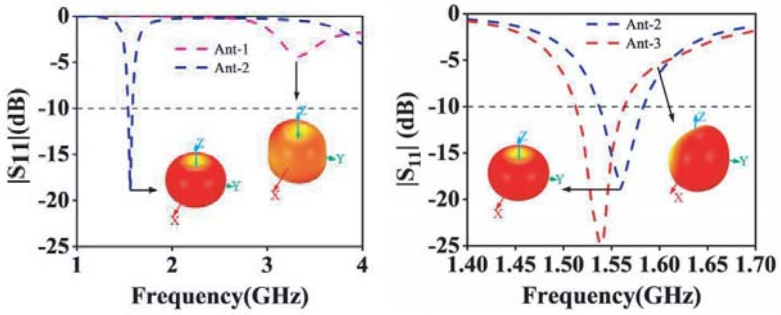

(a) (b)

Figure 3. The reflection coefficient and 3-D radiation pattern for Ant-1, Ant-2 and Ant-3.

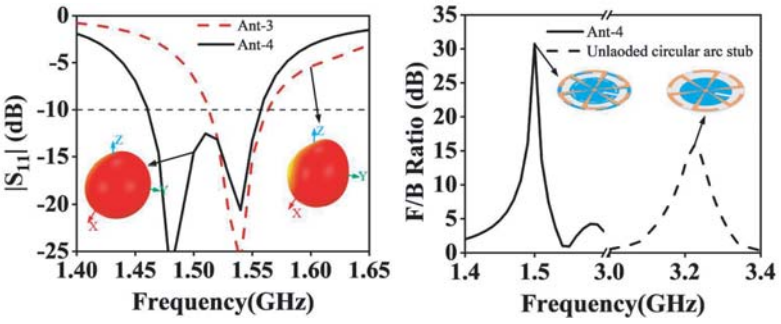

(a) (b)

Figure 4. The reflection coefficient, 3-D radiation pattern and F/B ratio for Ant-3, Ant-4, and unloaded circular arc stub antenna.

radiates more uniformly is formed by the dual side printed loop technique as shown in Fig. 2(b). Its center frequency shifts down to 1.55 GHz, and the overall size is reduced by 77% from $0.65\lambda_0 \times 0.65\lambda_0$ to $0.31 \times 0.31\lambda_0$. For Ant-3, a rectangular slot is etched on the ground plane of Ant-2, and it can change the current distribution on the ground plane to introduce an equivalent electric dipole, which combines with the equivalent magnetic dipole to obtain the endfire radiation pattern. As shown in Fig. 3(b), Ant-3 can achieve a good endfire radiation pattern at 1.6 GHz, but the impedance is not well matched. For Ant-4, six circular arc slots with rotational symmetry are etched on the ground plane of Ant-3. With reference to Fig. 4(a), compared with Ant-3, the center frequency further shifts down to 1.5 GHz, and the impedance matching has been obviously improved, while good endfire radiation characteristics are

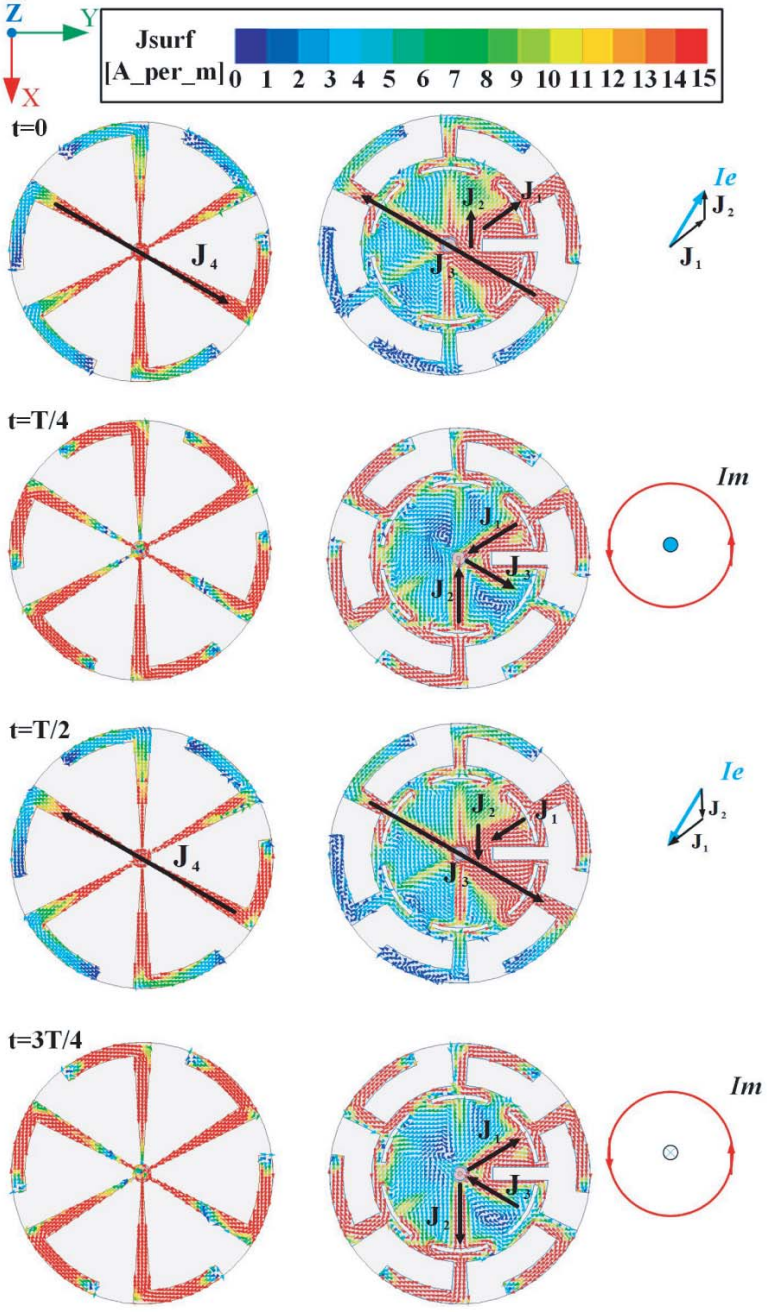

Figure 5. Current distribution of Ant-4 in a T period at 1.5 GHz.

maintained. Furthermore, Ant-4 has a very compact size with a radius of $0.148\lambda_0$ only ($ka = 0.93 < 1$ at 1.5 GHz). As shown in Fig. 4(b), the F/B ratios of Ant-4 (with dual side printed loop) and unloaded circular arc stub antenna (with one side printed loop) are 31.6 dB and 15.8 dB, respectively. Ant-4 has much higher F/B ratio because the dual side printed dipole produces an equivalent magnetic dipole with more uniform radiation. The simulated peak realized gain and radiation efficiencies (RE) of Ant-4 at 1.5 GHz are 4.63 dBi and 98.9%, respectively.

To further analyze the operating principle of the designed electrically small antenna with endfire characteristics, Fig. 5 shows the current distribution of Ant-4 at different time points at 1.5 GHz. The total current is equivalent to an electric dipole along the direction of $\phi = 150°$ at $t = 0$ and $t = T/2$. The total current appears as a loop current at $t = T/4$ and $t = 3T/4$. There is a 90° phase difference between the equivalent electric dipole and the loop current. In addition, there exists an inherent 90° phase difference between loop current and its equivalent z-directional magnetic dipole [14]. As a result, a total 180° phase difference is obtained between the equivalent electric dipole along $\phi = 150°$ direction and z-directional magnetic dipole. Therefore, the endfire radiation pattern along the direction of $\phi = 60°$ is obtained. Furthermore, the excitation magnitude ratio between the equivalent electric and magnetic dipoles has a strong influence on the F/B ratio. If the excitation magnitude ratio is close to 1, the F/B ratio is theoretically infinity [15]. A high F/B ratio can be obtained by adjusting the parameters of Ant-4, but these parameters will also affect impedance matching. Therefore, there were minor tradeoffs between the peak F/B ratio and the degree of matching when geometry parameters are adjusted. After antenna optimization, the radiation pattern of Ant-4 at 1.5 GHz is shown in Fig. 6. The radiation main beam points to the $\phi = 66°$ direction, slightly offsets from the theoretical direction, which is caused by stray current.

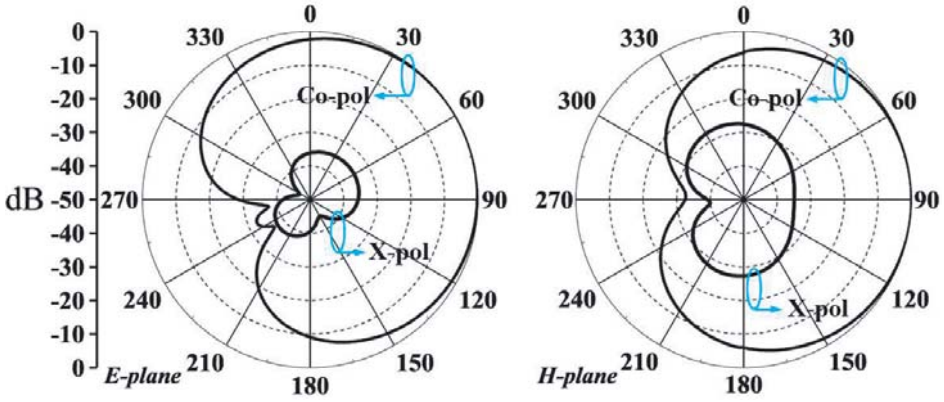

Figure 6. The simulated radiation patterns of Ant-4 at 1.5 GHz.

2.3. Reconfigurable Electrically Small Endfire Radiation Antenna Design

In order to achieve six switchable endfire radiation patterns, other five rectangular slots are etched on the ground plane of Ant-4 and six sets of biasing circuits integrated in the six rectangular slots as shown in Fig. 7. Each set of biasing circuits consists of an inductor, a capacitor, a PIN diode, a pad, and a printed dc line. The inductor and capacitor are used to isolate the radio frequency (RF) signal and dc signal. After optimization, the proposed pattern-reconfigurable ESA that has a more compact size with a radius of $0.14\lambda_0$ only ($ka = 0.87 < 1$ at 1.5 GHz) is obtained. Six switchable equivalent electric dipoles with rotational symmetric are introduced by using six PIN diodes. The six switchable electric dipoles combine with equivalent magnetic dipole to achieve six reconfigurable endfire radiation states, and the detailed information of the related states is listed in Table 2. The simulated 3-D radiation patterns for the six switchable endfire radiation states at 1.5 GHz are shown in Fig. 8. It can be seen that the six endfire radiation patterns have rotational symmetry and cover the whole 360° azimuth plane.

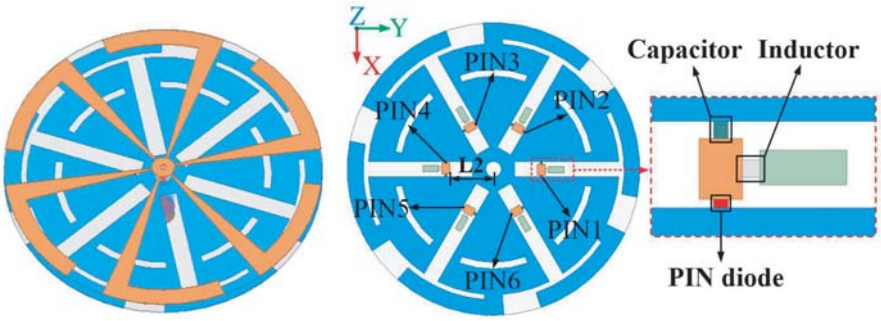

Figure 7. The structure and biasing circuits of the proposed antenna.

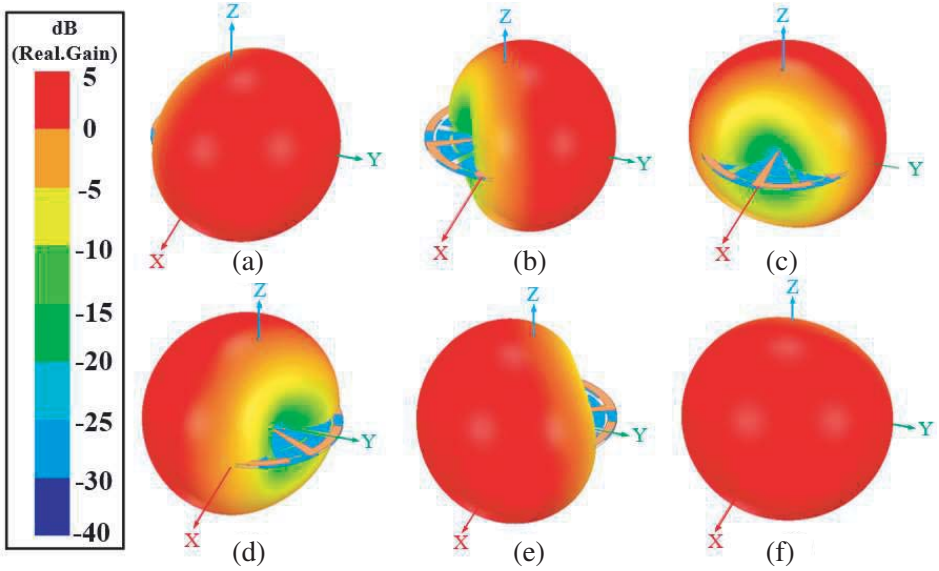

Figure 8. The simulated 3-D radiation pattern for the six endfire radiation states. (a) State A, (b) State B, (c) State C, (d) State D, (e) State E, (f) State F.

Table 2. Radiation states of the pattern-reconfigurable ESA.

State	PIN1	PIN2	PIN3	PIN4	PIN5	PIN6	Beam-direction
A	OFF	ON	ON	ON	ON	ON	64°
B	ON	OFF	ON	ON	ON	ON	124°
C	ON	ON	OFF	ON	ON	ON	184°
D	ON	ON	ON	OFF	ON	ON	244°
E	ON	ON	ON	ON	OFF	ON	304°
F	ON	ON	ON	ON	ON	OFF	4°

3. EXPERIMENTAL RESULTS

To verify the design, a prototype of the developed pattern-reconfigurable ESA was fabricated and measured. Figs. 9(a), (b), (c) are the bottom view of the prototype, biasing circuits, and the measurement environment, respectively. Six 47 nH inductors (LQW15A from Murata), six 10 pF capacitors (GRM155 from Murata), and six MACOM MA4GP907 PIN diodes [16] were used in the

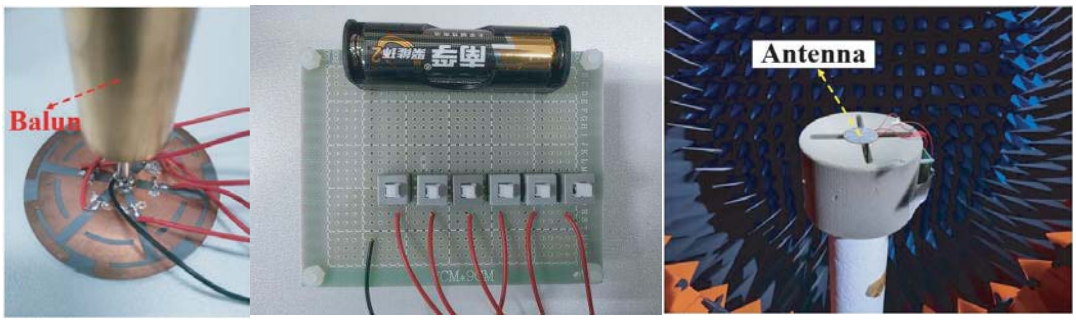

(a) (b) (c)

Figure 9. The antenna prototype: (a) bottom view, (b) biasing circuits, (c) antenna under test in the measurement chamber.

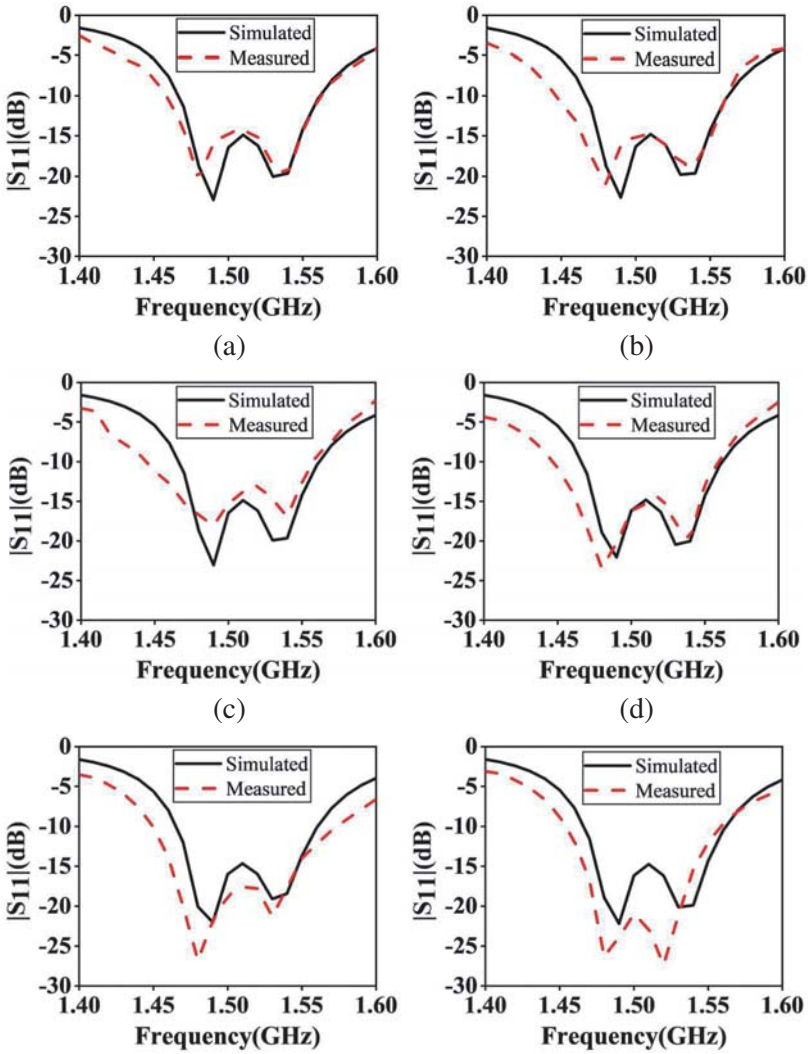

Figure 10. The simulated and measured reflection coefficient for the proposed antenna in its six states. (a) State A. (b) State B. (c) State C. (d) State D. (e) State E. (f) State F.

antenna prototype. A balun is used to prevent the leakage current from affecting the measured result [15]. A 1.5 V battery is used as dc source.

The measured and simulated reflection coefficients for the six endfire radiation states are shown in Fig. 10. The measured and simulated average −10 dB bandwidths are 7.3% and 6.7% in all states, respectively. There is a small frequency shift between simulated and measured results, which is mainly

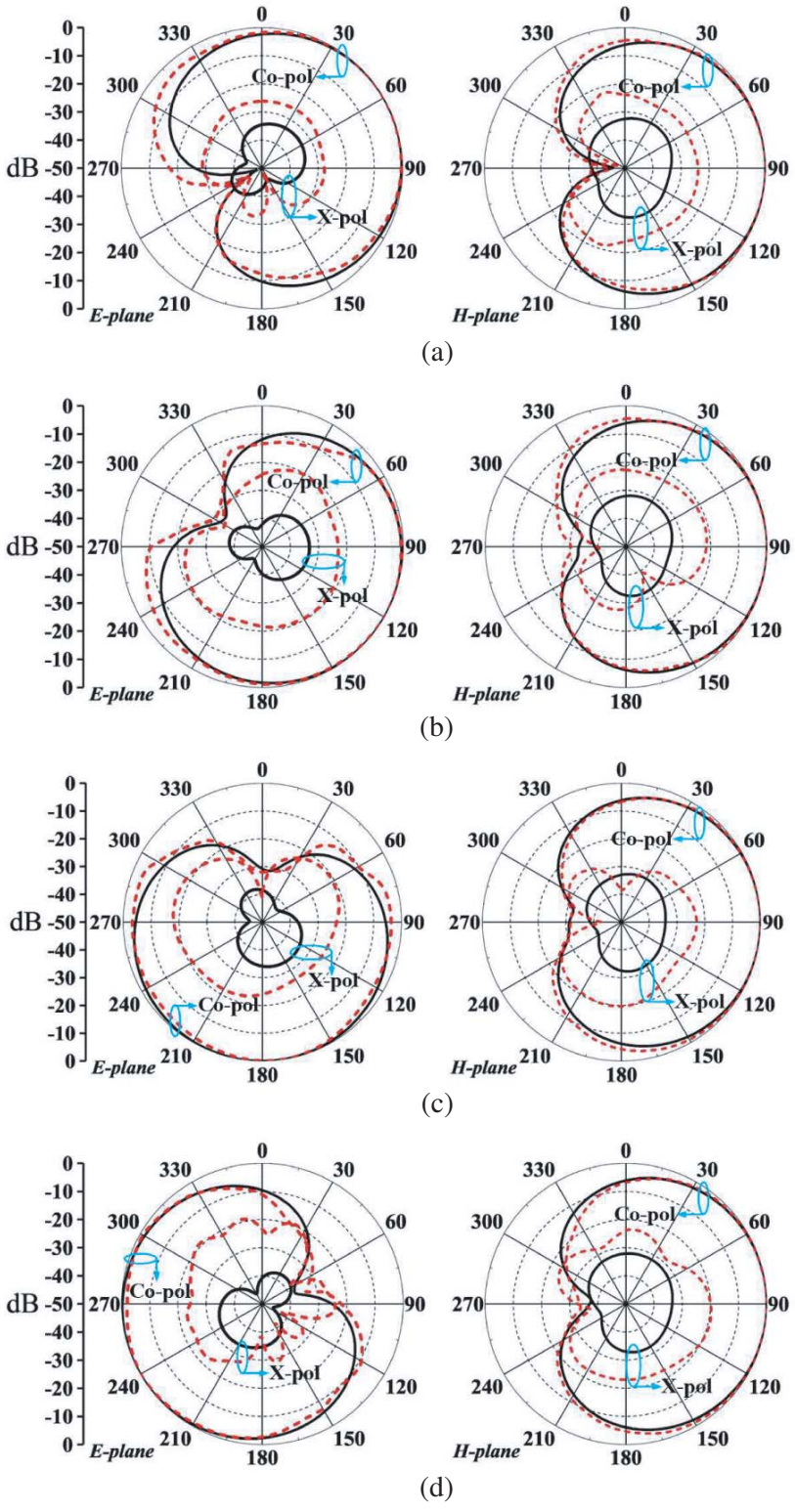

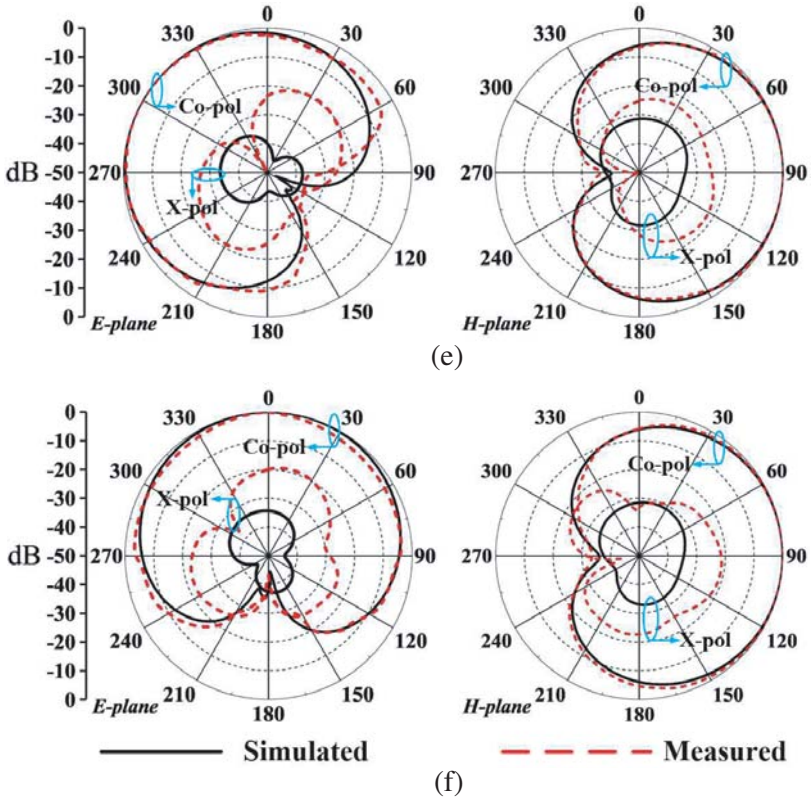

(e)

(f)

Figure 11. Measured and simulated radiation patterns of the six states in the E-plane and H-plane at 1.5 GHz. (a) State A. (b) State B. (c) State C. (d) State D. (e) State E. (f) State F.

caused by the tolerances in fabrication, assembly, and experiments, and simulation errors of lumped elements. The measured (simulated) average peak gain, F/B ratio, and RE values of six states at 1.5 GHz are $\sim$ 3.52 (4.18) dBi, $\sim$ 35.6 (39.8) dB, and $\sim$ 77.6 (86.1)%, respectively. The measured and simulated radiation patterns for State A-F are shown in Fig. 11. The measured average 3 dB beamwidths in the E-plane and H-plane for six states are about 138° and 130°, respectively, and the six switchable beams can fully cover the entire azimuthal plane. Fig. 12 shows the measured realized gains for six different biasing states, and the gain trends for all six states are almost the same.

Table 3 illustrates the comparison between the proposed pattern-reconfigurable ESA and published pattern-reconfigurable antenna. The proposed reconfigurable ESA has wider bandwidth (compared with most of the ESAs), most numbers of switchable states, and the highest F/B ratio. In addition,

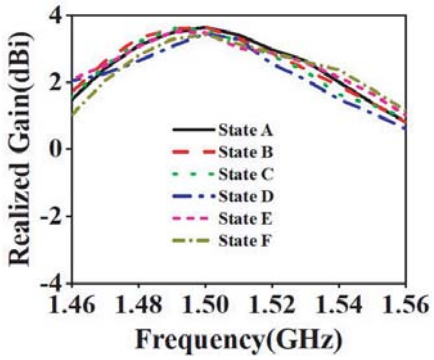

Figure 12. Measured realized gains of the proposed pattern-reconfigurable ESA.

Table 3. Comparison of the proposed antenna with published pattern-reconfigurable endfire radiation antenna.

Ref.	ka	FBW (%)	Peak gain (dBi)	Height	Switch. NO	Number of states	Covering space	RE (%)	Average F/B ratio (dB)
[5]	2.72	32.1	4.11	$0.0062\lambda_0$	4	4	360°	60	~ 10
[8]	2.12	10.9	7.13	$0.047\lambda_0$	3	3	360°	90	~ 10
[9]	1.32	15	3.5	$0.024\lambda_0$	4	4	360°	83	~ 25
[10]	0.6	2.7	8.5	$0.095\lambda_0$	2	2	220°	89.8	~ 7
[11]	0.92	2.73	3.59	$0.05\lambda_0$	3	3	360°	85	~ 18
[12]	0.94	12.9	4.43	$0.0007\lambda_0$	4	2	$< 220°$	70.5	~ 16.15
[13]	0.98	1.32	5.4	$0.0026\lambda_0$	2	3	$< 220°$	85	~ 13.3
This work	0.87	7.3	3.52	$0.005\lambda_0$	6	6	360°	77.6	~ 35.6

the proposed antenna also has the advantages of small electrical size, ultra-low-profile, and switchable endfire radiation patterns covering the entire 360° azimuth plane.

4. CONCLUSION

A pattern reconfigurable ESA with expanded bandwidth and high F/B ratio is presented in this paper. It consists of an Alford loop and a slotted ground with circular arc stubs. The Alford loop and loaded six circular arc stubs form a dual side printed loop, which can reduce the size by 77% compared with single side printed loop, and form an equivalent magnetic dipole that produces strong and uniform near magnetic field. The slotted ground with circular arc stubs can introduce six switchable equivalent electric dipoles by controlling the ON/OFF states of six PIN diodes, and they combine with the equivalent magnetic dipole to form six switchable endfire radiation patterns. The six endfire radiation patterns have rotational symmetry and cover the whole 360° azimuth plane. An antenna prototype operating at 1.5 GHz was fabricated and tested. The proposed antenna is electrically small ($ka = 0.87$) and has ultra-low profile ($0.005\lambda_0$). The measured peak realized gain and radiation efficiency are 3.52 dBi and 77.6%, respectively. In addition, compared with published pattern-reconfigurable endfire radiation ESAs, the proposed antenna has expanded bandwidth of 7.3% and highest F/B ratio of 35.6 dB.

ACKNOWLEDGMENT

This work was supported by the Key Project of Natural Science Foundation of Guangdong Province of China under Grant2018B030311013, the National Natural Science Foundation of China under Grant 61071056.

REFERENCES

1. Cidronali, A., S. Maddio, M. Passafiume, and G. Manes, "Car talk: Technologies for vehicle-to-roadside communications," *IEEE Microw. Mag.*, Vol. 17, No. 11, 40–60, Nov. 2016.
2. Li, Y. and K. Luk, "A multibeam end-fire magnetoelectric dipole antenna array for millimeter-wave applications," *IEEE Transactions on Antennas and Propagation*, Vol. 64, No. 7, 2894–2904, Jul. 2016.

3. Liu, F., Z. Zhang, W. Chen, Z. Feng, and M. F. Iskander, "An endfire beam-switchable antenna array used in vehicular environment," *IEEE Antennas and Wireless Propagation Letters*, Vol. 9, 195–198, 2010.
4. Zhong, L., J. Hong, and H. Zhou, "A novel pattern-reconfigurable cylindrical dielectric resonator antenna with enhanced gain," *IEEE Antennas and Wireless Propagation Letters*, Vol. 15, 1253–1256, Dec. 2016.
5. Jin, G., M. Li, D. Liu, and G. Zeng, "A simple planar pattern-reconfigurable antenna based on arc dipoles," *IEEE Antennas and Wireless Propagation Letters*, Vol. 17, No. 9, 1664–1668, Sept. 2018.
6. Zhang, T., S. Yao, and Y. Wang, "Design of radiation-pattern-reconfigurable antenna with four beams," *IEEE Antennas and Wireless Propagation Letters*, Vol. 14, 183–186, 2015.
7. Sabapathy, T., M. Jusoh, R. B. Ahmad, M. R. Kamarudin, and P. J. Soh, "A ground-plane-truncated, broadly steerable Yagi-Uda patch array antenna," *IEEE Antennas and Wireless Propagation Letters*, Vol. 15, 1069–1072, 2016.
8. Tang, M., Y. Duan, Z. Wu, X. Chen, M. Li, and R. W. Ziolkowski, "Pattern reconfigurable, vertically polarized, low-profile, compact, near-field resonant parasitic antenna," *IEEE Transactions on Antennas and Propagation*, Vol. 67, No. 3, 1467–1475, Mar. 2019.
9. Ouyang, J., Y. M. Pan, and S. Y. Zheng, "Center-fed unilateral and pattern reconfigurable planar antennas with slotted ground plane," *IEEE Transactions on Antennas and Propagation*, Vol. 66, No. 10, 5139–5149, Oct. 2018.
10. Lim, S. and H. Ling, "Design of electrically small, pattern reconfigurable Yagi antenna," *Electron. Lett.*, Vol. 43, No. 24, 1326–1327, Nov. 2007.
11. Tang, M., B. Zhou, and R. W. Ziolkowski, "Low-profile, electrically small, huygens source antenna with pattern-reconfigurability that covers the entire azimuthal plane," *IEEE Transactions on Antennas and Propagation*, Vol. 65, No. 3, 1063–1072, Mar. 2017.
12. Tang, M., B. Zhou, Y. Duan, X. Chen, and R. W. Ziolkowski, "Pattern-reconfigurable, flexible, wideband, directive, electrically small near-field resonant parasitic antenna," *IEEE Transactions on Antennas and Propagation*, Vol. 66, No. 5, 2271–2280, May 2018.
13. Wu, Z., M. Tang, M. Li, and R. W. Ziolkowski, "Ultralow-profile, electrically small, pattern-reconfigurable metamaterial-inspired huygens dipole antenna," *IEEE Transactions on Antennas and Propagation*, Vol. 68, No. 3, 1238–1248, Mar. 2020.
14. Balanis, C. A., *Antenna Theory: Analysis and Design*, 3rd Edition, Wiley, Hoboken, NJ, USA, 2005.
15. Tang, M.-C., H. Wang, and R. W. Ziolkowski, "Design and testing of simple, electrically small, low-profile, Huygens source antennas with broadside radiation performance," *IEEE Transactions on Antennas and Propagation*, Vol. 64, No. 11, 4607–4617, Nov. 2016.
16. MACOM, Products: MA4GP907, [Online], Available: http://cdn.macom.com/datasheets/MA4G-P907.pdf.